Electronic Supplementary Material (ESI) for Dalton Transactions.
This journal is © The Royal Society of Chemistry 2020

A Novel Sandwich shaped $\{Co^{III}_2Co^{II}_{12}Mo^{V}_{24}\}$ Cluster with Co^{II}_4 Triangle Core Encapsulated in Two Capped $Co^{III}Co^{II}_4Mo^{V}_{12}O_{40}$ Fragments

Hai-Ye Li,[a] Hua-Yu Pang,[a] Peng-Fei Yao,*[ab] Fu-Ping Huang,*[a] He-Dong Bian,[a] Fu-Pei Liang*[ac]

1. Experimental Section

2. Structural Section

3. Measurement Section

---

a State Key Laboratory for the Chemistry and Molecular Engineering of Medicinal Resources, School of Chemistry and Pharmacy, Guangxi Normal University, Guilin 541004, P. R. China. Fax: +86-773-2120958; E-mail: huangfp2010@163.com

b College of Chemistry and Environmental Engineering, Baise University, Baise, Guangxi 533000, P. R. China. yaopengfei1986@163.com

c Guangxi Key Laboratory of Electrochemical and Magnetochemical Functional Materials, College of Chemistry and Bioengineering, Guilin University of Technology, Guilin 541004, P. R. China. E-mail: fliangoffice@yahoo.com

1. Experimental Section

Materials and Physical Measurements

The reagents and solvents employed were commercially available and used as received without further purification. The C, H, and N microanalyses were carried out with a Perkin–Elmer PE 2400 II CHN elemental analyzer. The FT-IR spectra were recorded from KBr pellets in the range 4000-400 cm-1 on a Perkin–Elmer one FT-IR spectrophotometer. X-ray powder diffraction (XRPD) intensities were measured at 293 K on a Rigaku D/max-IIIA diffractometer (Cu-Kα, λ = 1.54056 Å). The crystalline powder samples were prepared by crushing the single-crystals and scanned from 3-65° at a rate of 5°/min. Calculated patterns of **1** were generated with PowderCell. TG-DTA tests were performed on a Perkin-Elmer thermal analyzer from room temperature to 800 °C under N_2 atmosphere at a heating rate of 5 °C/min. And the data were collected in positive ion mode. X-ray photoelectron spectroscopy (XPS) measurement was performed with a Kratos Axis Ultra DLD spectrometer. To further confirm the relative molar ratios of Co and Mo, the inductively coupled plasma mass spectrometry (ICP-MS) used for the elemental analyses of the metals in the bimetallic cluster were carried out with a PekinElmer FLexar-NexION 300X instrument. All magnetic measurements (solid state) were carried out on a Quantum Design MPMS-XL SQUID magnetometer in a temperature range of 2.0–300 K and a DC field of 1000 Oe. Data were corrected for the diamagnetic contribution calculated from Pascal constants and the diamagnetism of the sample and sample holder were taken into account.

Syntheses of complexes 1

$\{Co^{III}_2Co^{II}_{10}Cl_2(dpbt)_3(H_2O)_2[Co^{II}Mo^{V}_{12}O_{31}(CH_3O)_9]_2\}\cdot 24CH_3OH$ **(1).** A mixture containing 2,2′-H_2dbpt (87 mg, 0.3mmol), $CoCl_2\cdot 6H_2O$ (238 mg, 1mmol), $(NH_4)_6Mo_7O_{24}\cdot 4H_2O$ (247 mg, 0.2mmol), and triethylamine (0.5 mL) in methanol (15 mL) was stirred for 30 min in air, then transferred and sealed in an 25 mL Teflon-lined autoclave, which was heated at 160 °C for 3 days and then cooled to room temperature at a rate of 10 °C/h. Light-green flake-like crystals of **1** were obtained in 34 % yield. Elemental analysis for $C_{84}H_{174}Cl_2Co_{14}Mo_{24}N_{24}O_{106}$ (%) Calcd: C, 15.73; H, 2.73; N, 5.24. Found: C: 16.12; H: 2.52; N: 5.15 IR (KBr, cm^{-1}): 3405(s), 2926(m), 2824(m), 1612(s), 1460(m),1406(m), 1302(w), 1217(w), 1149(w), 1029(s), 951(s), 899(m), 794(s), 751(s), 594(w), 566(m), 525(m), 441(w), 416(w). It is worth mentioning that all the Mo atoms in the structure of **1** as Mo(V) while the starting material Mo(VI) salt and the Co(II) starting material oxidised partially to Co(III). The process of the assembly section of **1** is accompanied by complicated redox reaction. The dpbt ligand containing a large number of N atoms and/or the Co(II) starting material in the alkaline reaction environment could reduce Mo^{VI} to Mo^{V}. (Similar phenomenon can be found in the references: X.-L. Wang, C. Qin, E.-B. Wang, Z.-M. Su, Y.-G. Li, L. Xu, *Angew. Chem. Int. Ed.* 2006, **45**, 7411–7414. Y. Xu, J.-Q. Xu, K.-L. Zhang, Y. Zhang, X.-Z. You, *Chem. Commun.*, 2000, 153-154.)

X-ray Structure Determination.

Single-crystal X-ray diffraction data collection for **1** was conducted on an Agilent Supernova diffractometer (Mo, $\lambda = 0.71073$Å) at 100 K. The data was processed using CrysAlisPro. (Version 1.171.35.211). Preliminary orientation matrix and cell parameters were determined from three sets of scans at different starting angles. Data frames were obtained at scan intervals of 0.25° with an exposure time of 90 s per frame. The structure was solved by direct methods and refined by full-matrix least-squares refinements based on F^2 within the SHELXTL Program package. All the non-hydrogen atoms were refined anisotropically. Hydrogen atoms of water molecules were located in a difference Fourier map and refined isotropically in the final refinement cycles. Other hydrogen atoms were placed in calculated positions and refined by using a riding model. The final cycle of full matrix least-squares refinement was based on observed reflections and variable parameters. Solvent molecules in **1** are significantly disordered and could not be modeled properly due to the lack of well defined atomic positions, thus the SQUEEZE procedure implemented in Platon (Spek, A. L. J. Appl. Crystallogr. 2003, 36, 7; Vander Sluis, P.; Spek. A. L.

Acta Cryst. 1990. A46, 194) was used to calculate the solvent disorder area and remove its contribution to the overall intensity data. The Squeeze (or Bypass) procedure is a widely used and accepted method that corrects diffraction data for structures affected by the presence of heavily disordered solvent. However, the use of Squeeze does not impact the framework atoms. For **1**, SQUEEZE gives 1746 electrons/unit cell for the voids. If these electrons are all from CH_3OH (18 e^-), each unit cell has 97 (*ca.* 1746/18) CH_3OH molecules, and each formula unit has 24 CH_3OH molecules (since Z = 4). So the suitable formula for this compound should be $\{Co^{III}_2Co^{II}_{10}Cl_2(dpbt)_3(H_2O)_2[Co^{II}Mo^{V}_{12}O_{31}(CH_3O)_9]_2\}\cdot 24CH_3OH$. If other molecules (like H_2O or Et_3N) are mixed in the structure, it would become more complicated and not easy to assign them. Additionally, the elemental analysis and TG study for **1** approve the result. The crystallographic details are summarized in Table S1. Selected bond distances and bond angles are listed in Tables S2. The crystallographic data of **1** in CIF format have been deposited in the Cambridge Crystallographic Data Center (CCDC reference number 1881655). These data can be obtained free of charge via www.ccdc.cam.ac.uk/conts/retrieving.html; e-mail: deposit@ccdc.cam.ac.uk.

Mass Spectrometry Measurements

HRESI-MS measurements were conducted at a capillary temperature of 275 °C. Aliquots of the solution were injected into the device at 0.3 mL/h. The mass spectrometer used for the measurements was a ThermoExactive instrument, and the data were collected in positive and negative ion mode. The spectrometer was previously calibrated with the standard tune mix to give a precision of ca. 2 ppm in the region of m/z 400−2000. The capillary voltage was 50 V, the tube lens voltage was 150 V, and the skimmer voltage was 25 V. The in-source energy was set to a range of 0 eV with a gas flow rate at 10% of the maximum.

2. Structural Section

Table S1 Crystal data and structure refinement for 1

Compound	**1 (Squeezed)**
Empirical formula	$C_{60}H_{78}Cl_2Co_{14}Mo_{24}N_{24}O_{82}$
Formula weight (*M*)	5645.94

Crystal system	orthorhombic
Space group	Pbcn
a (Å)	36.6408 (18)
b (Å)	22.3598 (9)
c (Å)	22.750 (2)
α (°)	90.00
β (°)	90.00
γ (°)	90.00
V/(Å ^{3})	18639 (2)
Z	4
D_c(g cm^{-3})	2.012
F(000)	10728
θ range for data collection (°)	2.9–25.3
Reflections collected / unique	57283/16851 [R(int) = 0.0542]
Goodness-of-fit on F^2	1.033
Final R indices [$I > 2\sigma(I)$]	$R_1 = 0.0549$ $\omega R_2 = 0.1481$
R indices (all data)	$R_1 = 0.0815$ $\omega R_2 = 0.1601$

Table S2 Selected Atomic Distances (Å) and Bond Angles (deg) for complexes 1

1. (Symmetry code: (A) $-x$, y, $-z$+1/2.)

Co1—O1	2.031 (5)	Co3—O9A	2.024 (5)
Co1—O2	2.019 (5)	Co3—O9	2.024 (5)
Co1—O3	2.025 (5)	Co3—N4A	2.057 (7)
Co1—O4	2.003 (4)	Co3—N4	2.057 (7)
Co2—O5	2.038 (5)	Co4—O8	2.124 (4)
Co2—O21	2.066 (5)	Co4—O8A	2.124 (4)
Co2—O22	2.041 (5)	Co4—O9	2.129 (5)
Co2—N3	2.028 (7)	Co4—O9A	2.129 (5)
Co2—N1	2.165 (5)	Co4—O11A	2.119 (4)
Co5—O7A	2.349 (5)	Co4—O11	2.119 (4)
Co5—O8A	2.063 (4)	Co6—O20	2.022 (5)
Co5—O11	2.069 (4)	Co6—O36	2.018 (5)
Co5—O12	2.344 (5)	Co6—O38	2.032 (5)
Co5—N7	2.078 (6)	Co6—N5	2.160 (6)
Co5—N11A	2.091 (6)	Co6—N6	2.035 (6)
Co7—Cl1	2.198 (3)	Co8—O6	2.211 (5)
Co7—O23	1.943 (6)	Co8—O13	2.062 (4)
Co7—O25	1.977 (6)	Co8—O14	2.134 (6)
Co7—O35	1.982 (5)	Co8—O15	2.041 (5)
Co8—N9	2.217 (6)	Co8—N10	2.044 (6)
Mo1—O3	2.228 (5)	Mo2—O4	2.174 (4)
Mo1—O5	2.003 (5)	Mo2—O5	1.947 (5)
Mo1—O6	1.935 (5)	Mo2—O6	1.950 (5)

Mo1—O29	2.092 (5)	Mo2—O7	1.718 (5)
Mo1—O30	1.685 (5)	Mo2—O8	2.095 (4)
Mo1—O41	2.078 (5)	Mo2—O9	2.089 (5)
Mo3—O4	2.191 (5)	Mo4—O2	2.201 (5)
Mo3—O8	2.045 (4)	Mo4—O13	1.976 (5)
Mo3—O11	2.087 (5)	Mo4—O31	2.099 (5)
Mo3—O12	1.710 (5)	Mo4—O32	2.123 (5)
Mo3—O13	1.944 (4)	Mo4—O33	1.703 (5)
Mo3—O38	1.962 (5)	Mo4—O38	1.925 (5)
Mo5—O2	2.206 (5)	Mo6—O3	2.198 (5)
Mo5—O15	1.946 (5)	Mo6—O15	1.944 (5)
Mo5—O23	1.958 (5)	Mo6—O16	1.686 (5)
Mo5—O24	2.103 (5)	Mo6—O23	1.993 (5)
Mo5—O32	2.103 (5)	Mo6—O40	2.111 (6)
Mo5—O37	1.692 (5)	Mo6—O41	2.095 (5)
Mo7—O2	2.189 (5)	Mo8—O1	2.188 (5)
Mo7—O17	1.681 (5)	Mo8—O18	1.686 (5)
Mo7—O24	2.100 (5)	Mo8—O34	2.106 (6)
Mo7—O31	2.112 (5)	Mo8—O35	1.958 (6)
Mo7—O35	1.968 (6)	Mo8—O36	1.933 (5)
Mo7—O36	1.943 (5)	Mo8—O39	2.083 (6)
Mo9—O1	2.185 (5)	Mo10—O1	2.214 (5)
Mo9—O22	1.945 (6)	Mo10—O19	1.671 (6)
Mo9—O25	1.963 (6)	Mo10—O20	1.986 (5)
Mo9—O26	2.104 (6)	Mo10—O21	1.948 (5)
Mo9—O27	1.693 (6)	Mo10—O26	2.105 (6)
Mo9—O34	2.114 (6)	Mo10—O39	2.085 (5)
Mo11—O4	2.205 (5)	Mo12—O3	2.160 (5)
Mo11—O9	2.111 (5)	Mo12—O22	1.951 (5)
Mo11—O10	1.717 (5)	Mo12—O25	1.961 (6)
Mo11—O11	2.045 (5)	Mo12—O28	1.679 (5)
Mo11—O20	1.961 (5)	Mo12—O29	2.094 (6)
Mo11—O21	1.973 (5)	Mo12—O40	2.096 (6)
Mo1—Mo2	2.5935 (9)	Mo3—Mo4	2.6194 (9)
Mo5—Mo6	2.6097 (11)	Mo7—Mo8	2.6182 (12)
Mo9—Mo12	2.6101 (12)	Mo10—Mo11	2.6190 (9)
O2—Co1—O1	108.8 (2)	O8—Co4—O8A	109.3 (3)
O2—Co1—O3	109.1 (2)	O8A—Co4—O9	163.21 (18)
O3—Co1—O1	108.2 (2)	O8—Co4—O9A	163.21 (18)
O4—Co1—O1	109.8 (2)	O8—Co4—O9	81.48 (17)
O4—Co1—O2	110.1 (2)	O8A—Co4—O9A	81.48 (17)
O4—Co1—O3	110.85 (19)	O9—Co4—O9A	91.3 (3)
O5—Co2—O21	86.7 (2)	O11—Co4—O8	80.38 (17)
O5—Co2—O22	90.6 (2)	O11A—Co4—O8A	80.38 (17)

O5—Co2—N1	153.5 (2)	O11—Co4—O8A	88.87 (17)
O21—Co2—N1	119.8 (2)	O11A—Co4—O8	88.87 (17)
O22—Co2—O21	88.8 (2)	O11A—Co4—O9	113.45 (18)
O22—Co2—N1	89.5 (2)	O11—Co4—O9	80.08 (18)
N3—Co2—O5	107.2 (2)	O11A—Co4—O9A	80.08 (18)
N3—Co2—O21	86.0 (2)	O11—Co4—O9A	113.45 (18)
N3—Co2—O22	161.0 (3)	O11—Co4—O11A	161.4 (3)
N3—Co2—N1	77.4 (3)	O8A—Co5—O7A	73.39 (17)
O9A—Co3—O9	97.6 (3)	O8A—Co5—O11	91.95 (17)
O9A—Co3—N4A	90.5 (2)	O8A—Co5—O12	87.92 (17)
O9—Co3—N4	90.5 (2)	O8A—Co5—N7	171.8 (2)
O9—Co3—N4A	170.7 (2)	O8A—Co5—N11A	97.2 (2)
O9A—Co3—N4	170.7 (2)	O11—Co5—O7A	91.51 (18)
N4—Co3—N4A	81.7 (4)	O11—Co5—O12	72.81 (18)
O20—Co6—O38	90.0 (2)	O11—Co5—N7	93.9 (2)
O20—Co6—N5	136.3 (2)	O11—Co5—N11A	170.3 (2)
O20—Co6—N6	101.7 (2)	O12—Co5—O7A	155.35 (17)
O36—Co6—O20	93.7 (2)	N7—Co5—O7A	100.7 (2)
O36—Co6—O38	92.0 (2)	N7—Co5—O12	99.3 (2)
O36—Co6—N5	88.8 (2)	N7—Co5—N11A	76.6 (2)
O36—Co6—N6	164.1 (2)	N11A—Co5—O7A	88.0 (2)
O38—Co6—N5	133.5 (2)	N11A—Co5—O12	110.6 (2)
O38—Co6—N6	91.7 (2)	O6—Co8—N9	112.7 (2)
N6—Co6—N5	77.5 (2)	O13—Co8—O6	81.13 (18)
O23—Co7—Cl1	118.27 (19)	O13—Co8—O14	83.8 (2)
O23—Co7—O25	98.0 (2)	O13—Co8—N9	164.3 (2)
O23—Co7—O35	97.1 (2)	O14—Co8—O6	158.9 (2)
O25—Co7—Cl1	121.72 (19)	O14—Co8—N9	84.5 (2)
O25—Co7—O35	96.7 (2)	O15—Co8—O6	82.79 (19)
O35—Co7—Cl1	119.79 (18)	O15—Co8—O13	90.06 (19)
O15—Co8—O14	111.9 (2)	N10—Co8—O13	116.1 (2)
O15—Co8—N9	84.7 (2)	N10—Co8—O14	94.8 (2)
O15—Co8—N10	144.8 (2)	N10—Co8—N9	75.3 (2)
N10—Co8—O6	78.9 (2)		

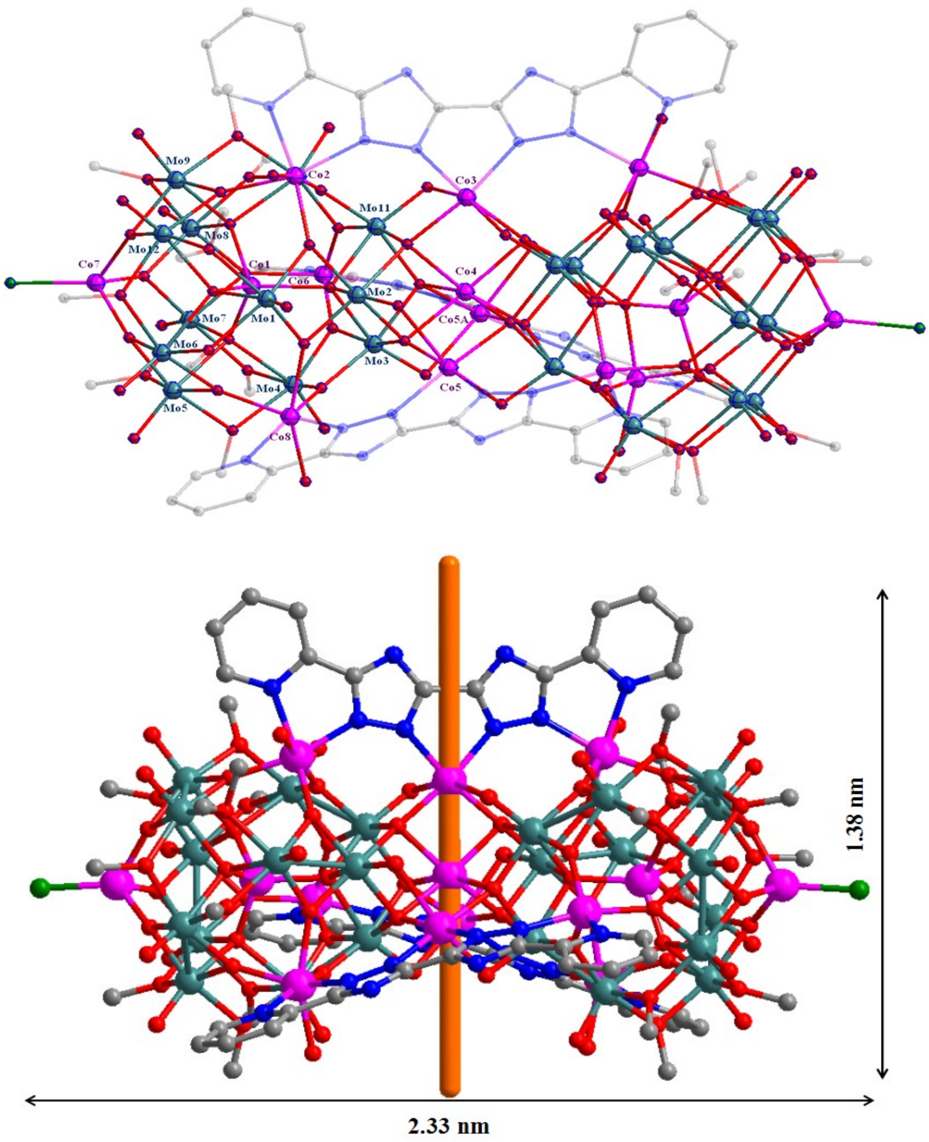

Fig. S1 The coordination environment of the Co(II)/Co(III) and Mo(V) atoms in the $\{Co_{14}Mo_{24}\}$ nanocluster of **1**

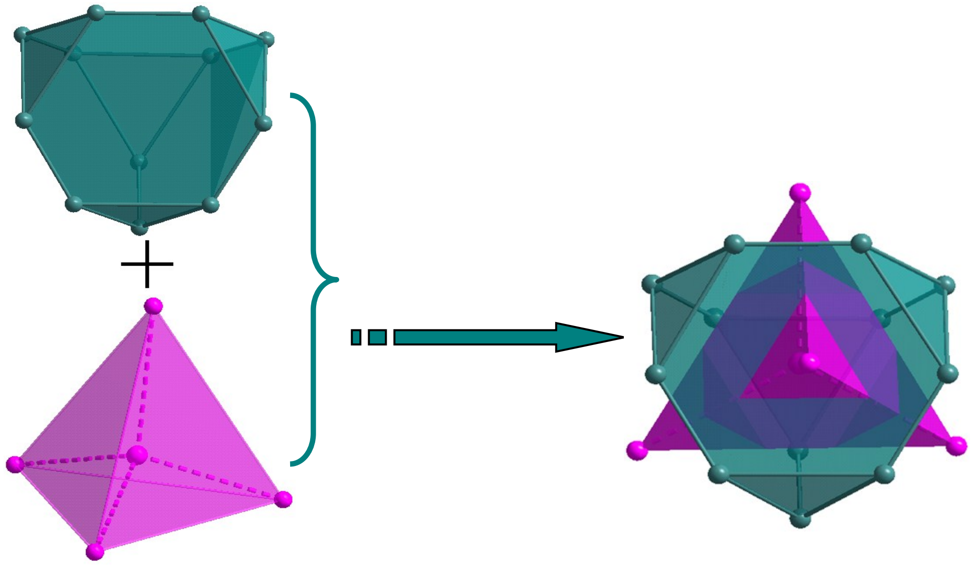

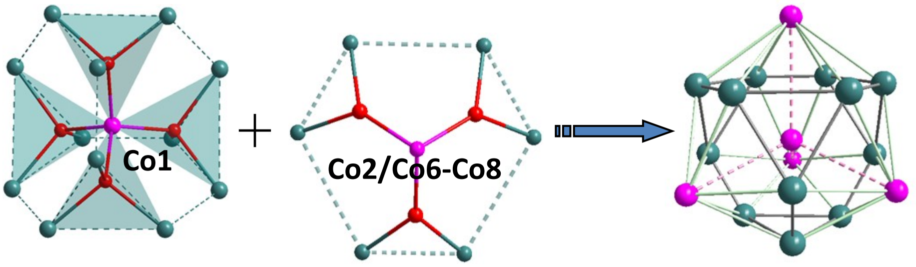

Fig. S2 The $\{Co_5Mo_{12}\}$ fragments in **1** highlighting the distorted truncated tetrahedron Mo_{12} with a body-centered Co_5 tetrahedron. The inner Co1 atom bridged by μ_4-O atoms, and the ambient Co (Co2/Co6/Co7/Co8) atoms bridged by μ_3-O atoms with Mo atoms, respectively.

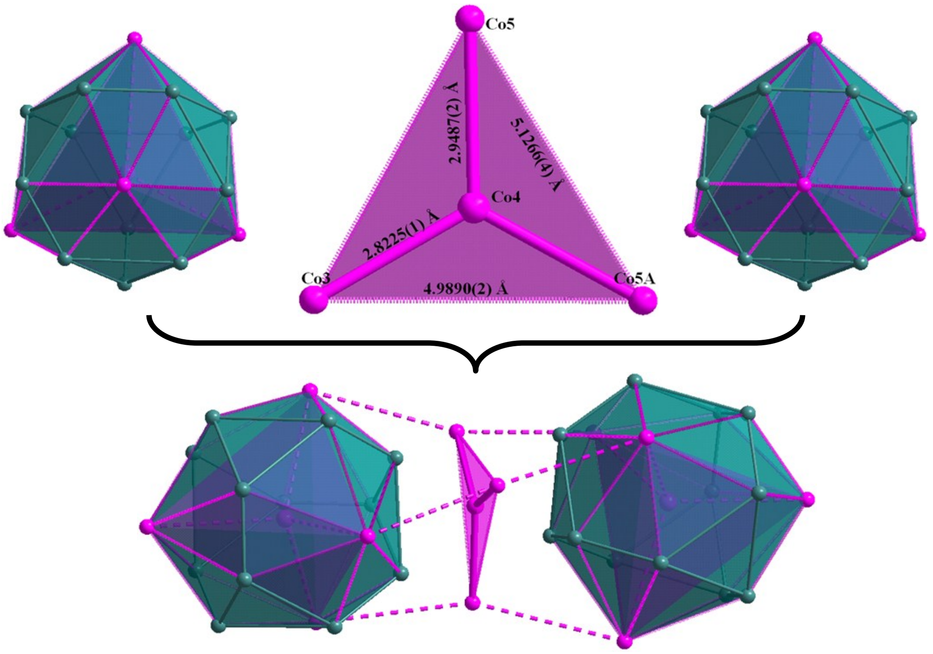

Fig. S3 The overall $\{Co_{12}Mo_{24}\}$ skeleton constructed by a equicrural triangle (highlight) of the Co_4 core and two $[Co_5Mo_{12}]$ fragments.

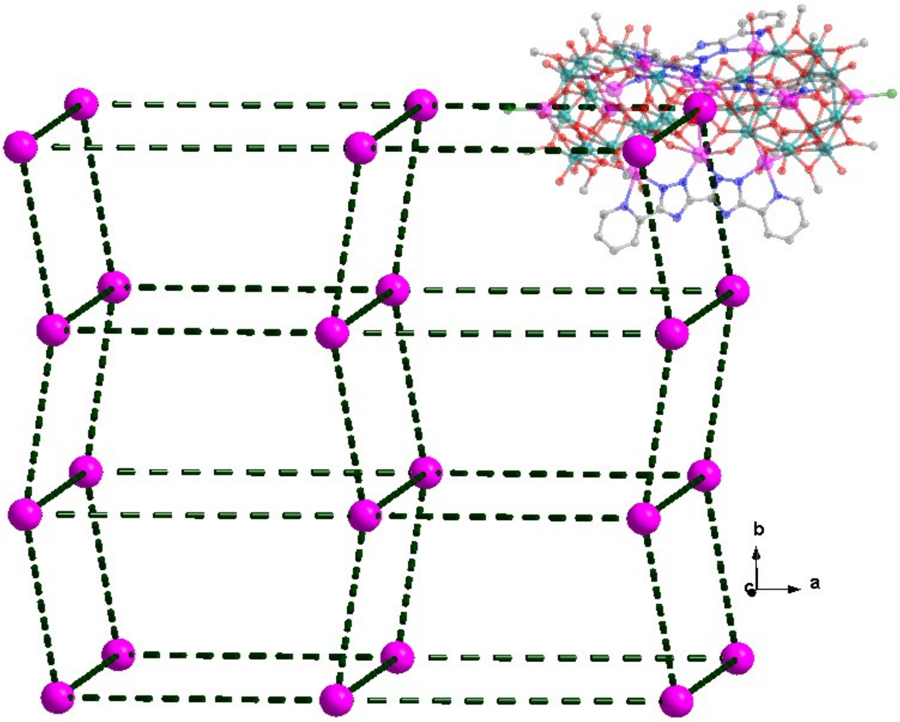

Fig. S4 the packing-diagram of the supramolecular balls (purple spheres) of **1** in the lattice.

3. Measurement Section

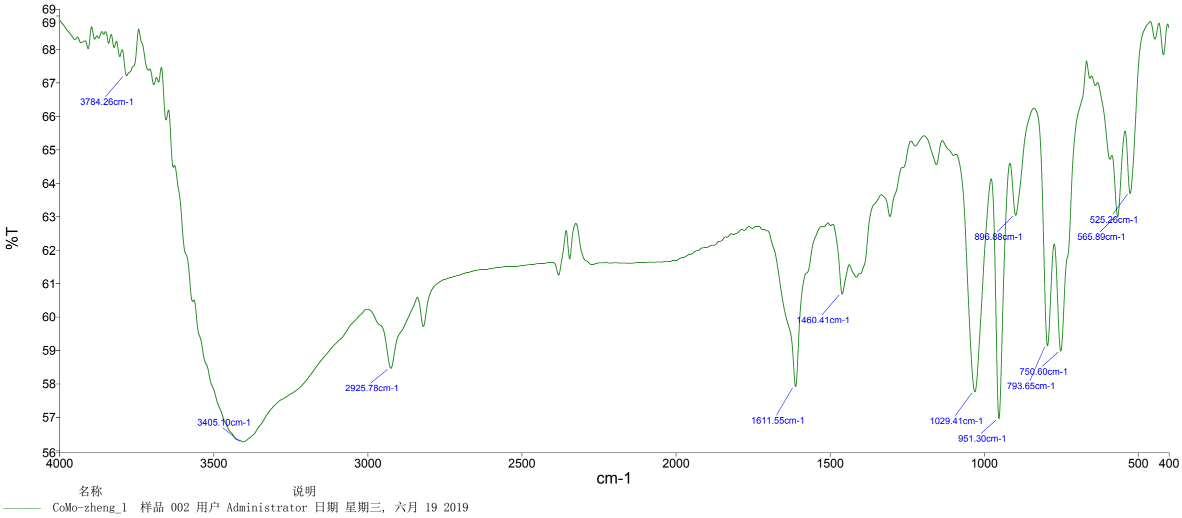

Fig. S5 The IR spectroscopy of **1**.

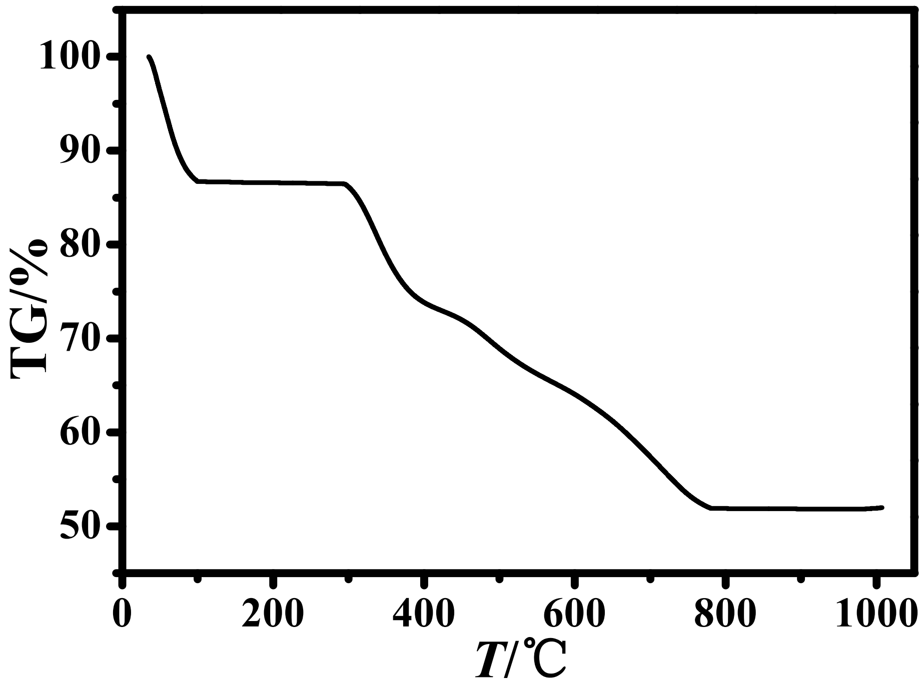

Fig. S6 TGA curves for compound **1**.

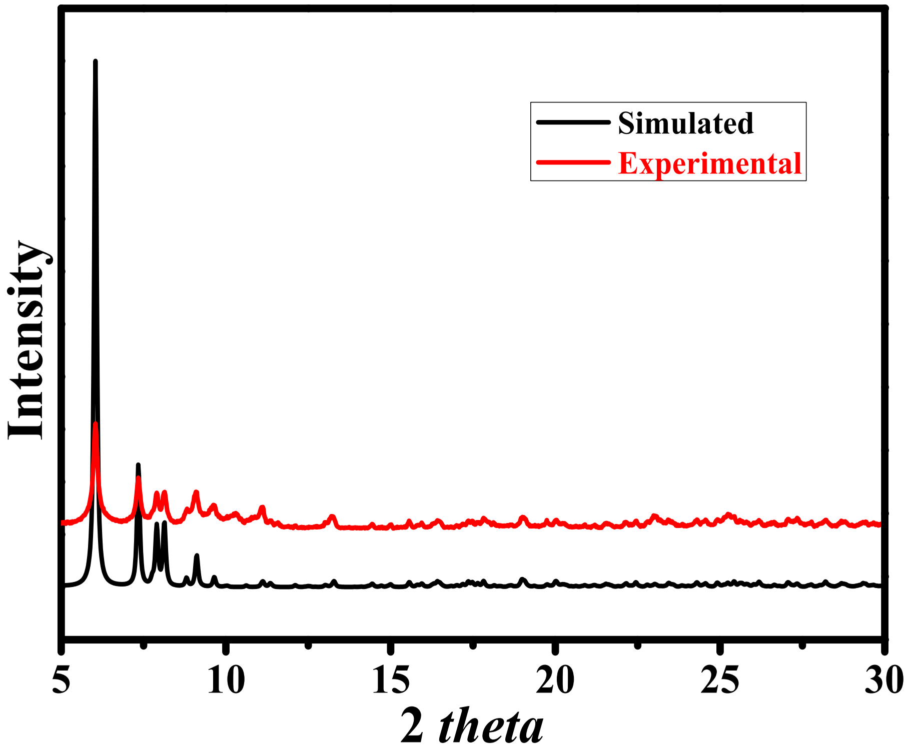

Fig. S7 Measured and calculated powder X-ray diffraction (PXRD) pattern of **1**. The PXRD pattern is the same as those simulated from the single crystal structure determinations, indicating the phase purity of the products, the differences in intensities may be due to the preferred orientation of the powder samples.

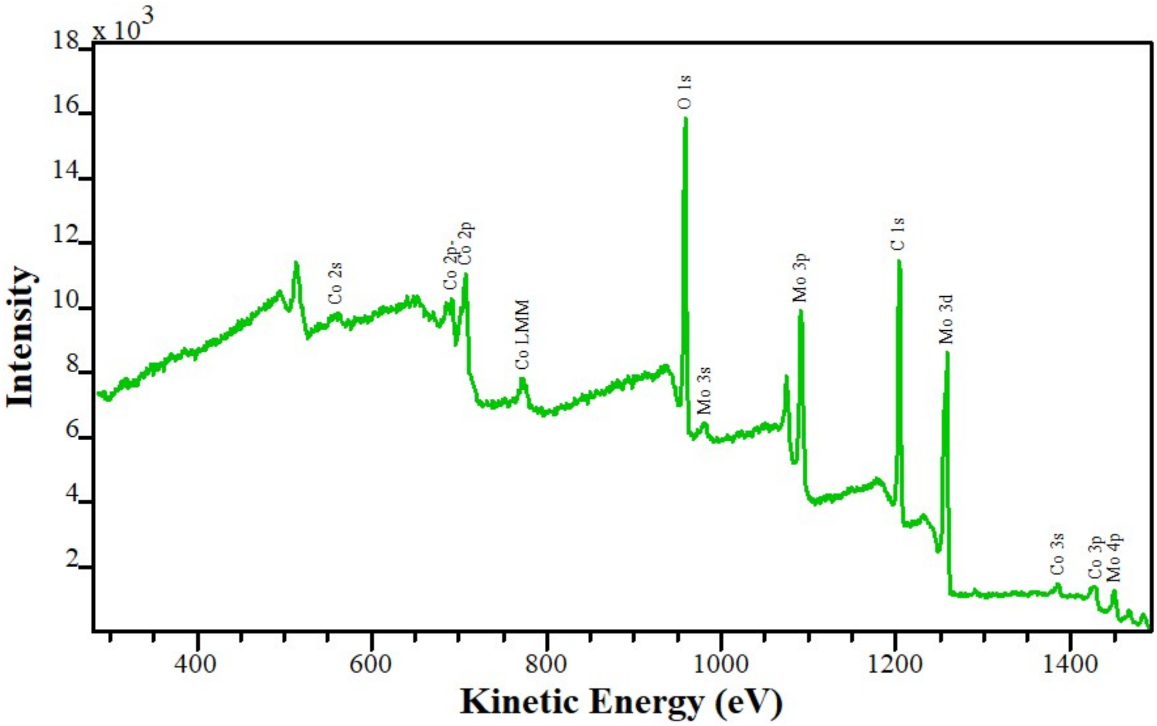

Fig. S8 The XPS spectrum of **1**.

Table S3. The Peak assignments of the ESI-MS spectra of F1-F3

Fragments	formula		m/z	
			Observed	Calculated
F1	$[Co^{III}_2Co^{II}_{12}Mo^{V}_{24}O_{62}Cl_2(dpbt)_3(H_2O)_2(CH_3O)_x(OH)_{18-x}-2H]^{2-}$	X=9	2761.937	2761.950
		X=10	2768.960	2768.958
		X=11	2776.010	2775.966
		X=12	2782.989	2782.973
		X=13	2789.995	2789.981
		X=14	2797.026	2796.989
		X=15	2803.985	2803.997
		X=16	2810.970	2811.005
		X=17	2817.980	2818.013
		X=18	2825.017	2825.020
F2	$[Co^{III}_2Co^{II}_{12}Mo^{V}_{24}O_{62}Cl_2(dpbt)_3(H_2O)_2(CH_3O)_x(OH)_{19-x}-2H]^{3-}$	X=6	1831.939	1831.947
		X=7	1836.945	1836.952
		X=8	1841.601	1841.624
		X=9	1846.275	1846.296
		X=10	1850.967	1850.967
		X=11	1855.623	1855.639
		X=12	1860.296	1860.311
		X=13	1864.988	1864.983
F3	$[Co^{III}Mo^{V}_7O_{20}+H]^-$		1051.183	1051.180

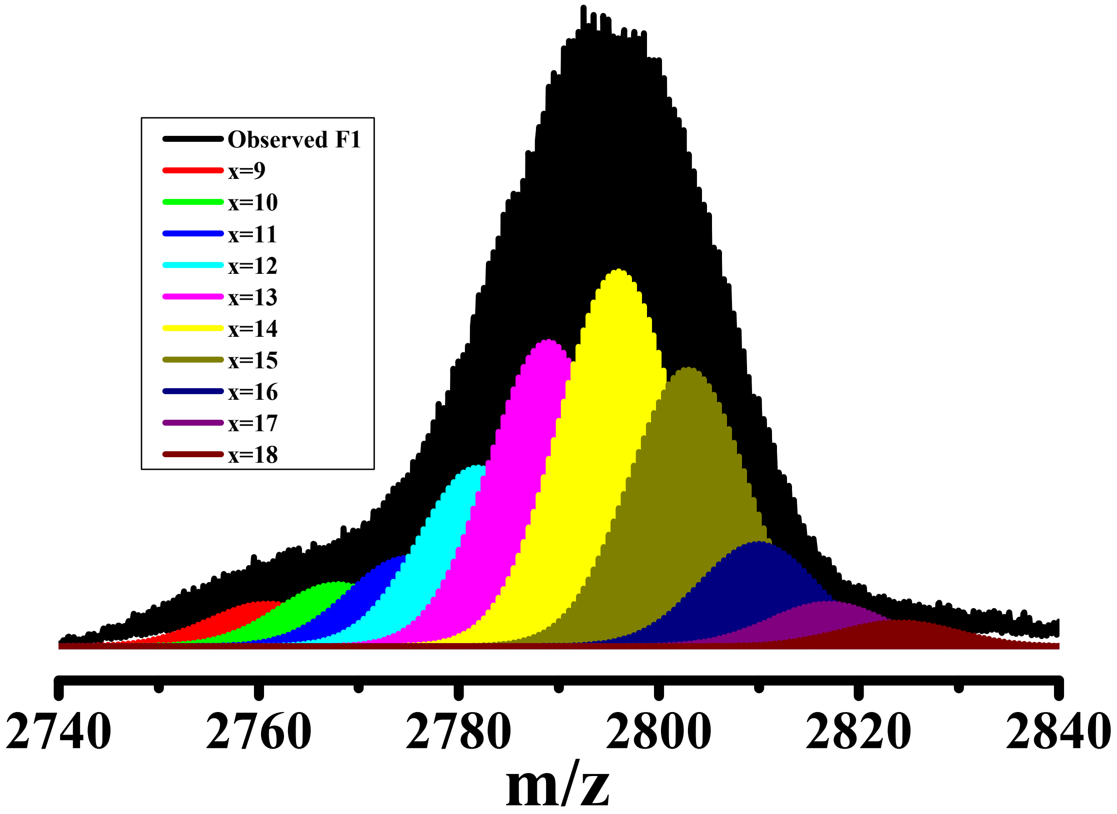
Observed F1
x=9
x=10
x=11
x=12
x=13
x=14
x=15
x=16
x=17
x=18
2740
2760
2780
2800
2820
2840
m/z

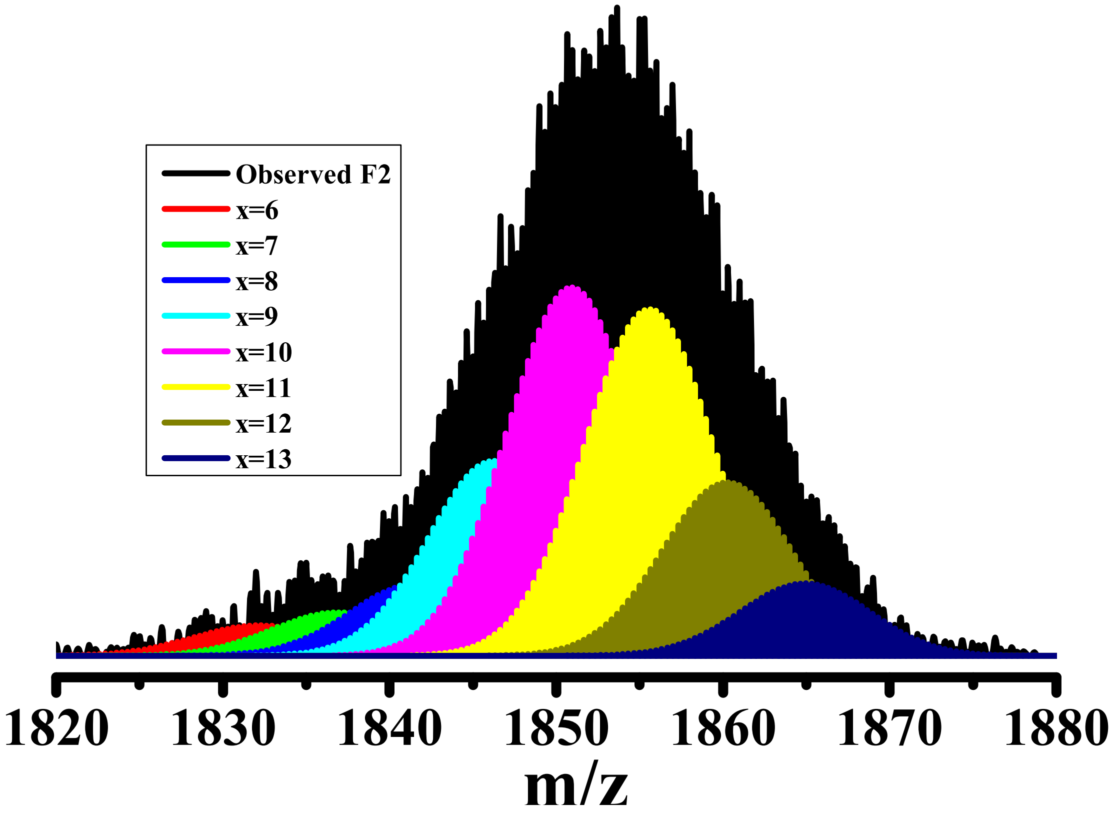
Observed F2
x=6
x=7
x=8
x=9
x=10
x=11
x=12
x=13
1820
1830
1840
1850
1860
1870
1880
m/z

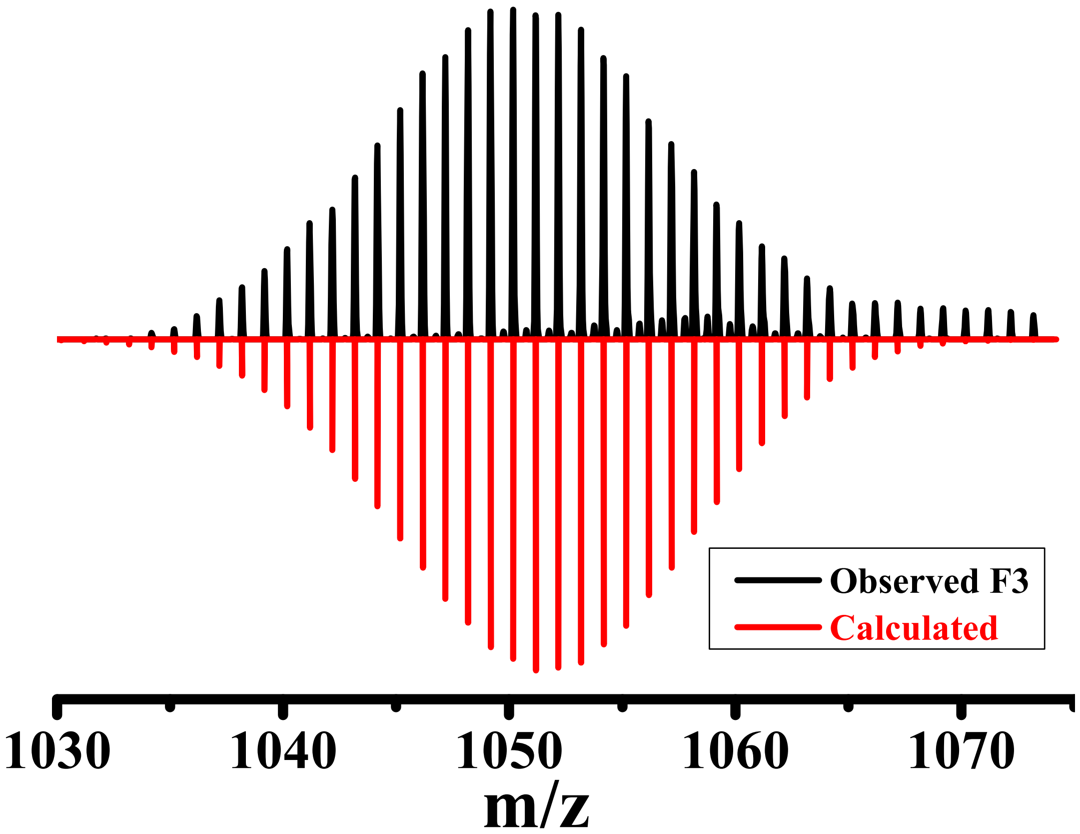

Fig. S9 The superposed simulated and observed spectra of F1-F3 Fragments at the in-source energy of 0 eV.

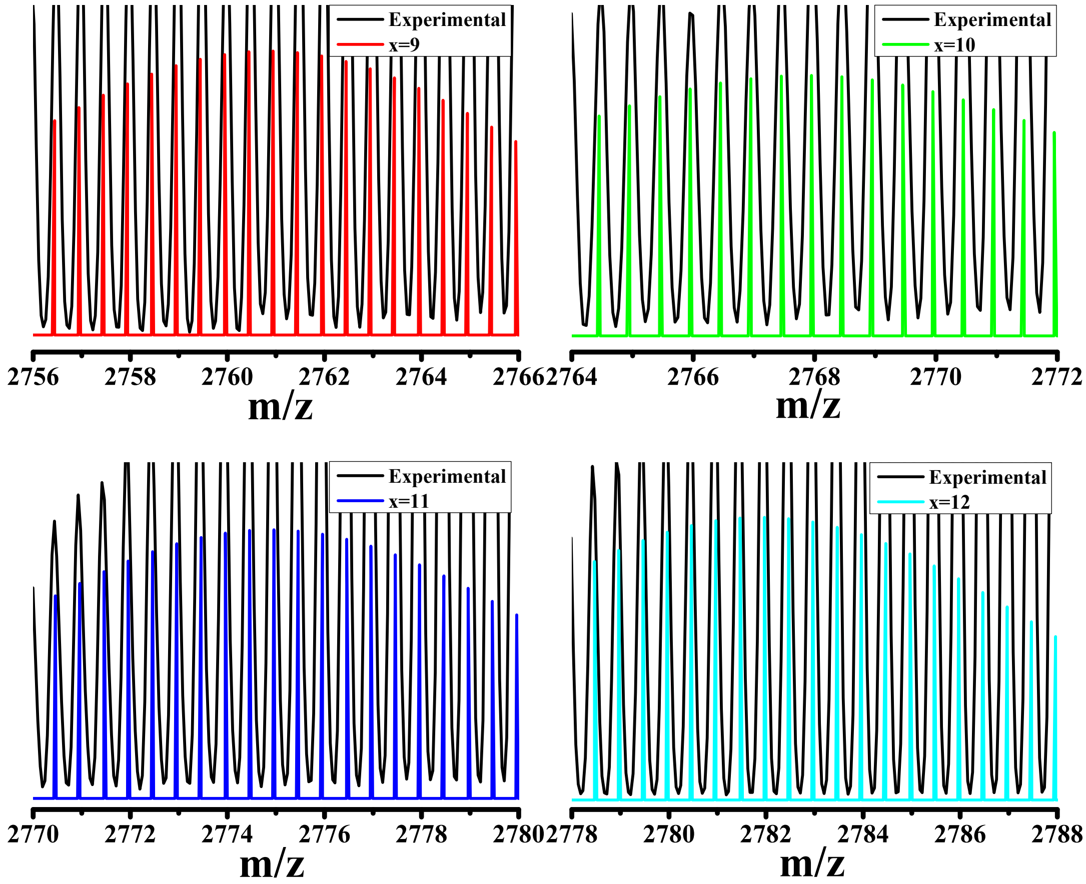

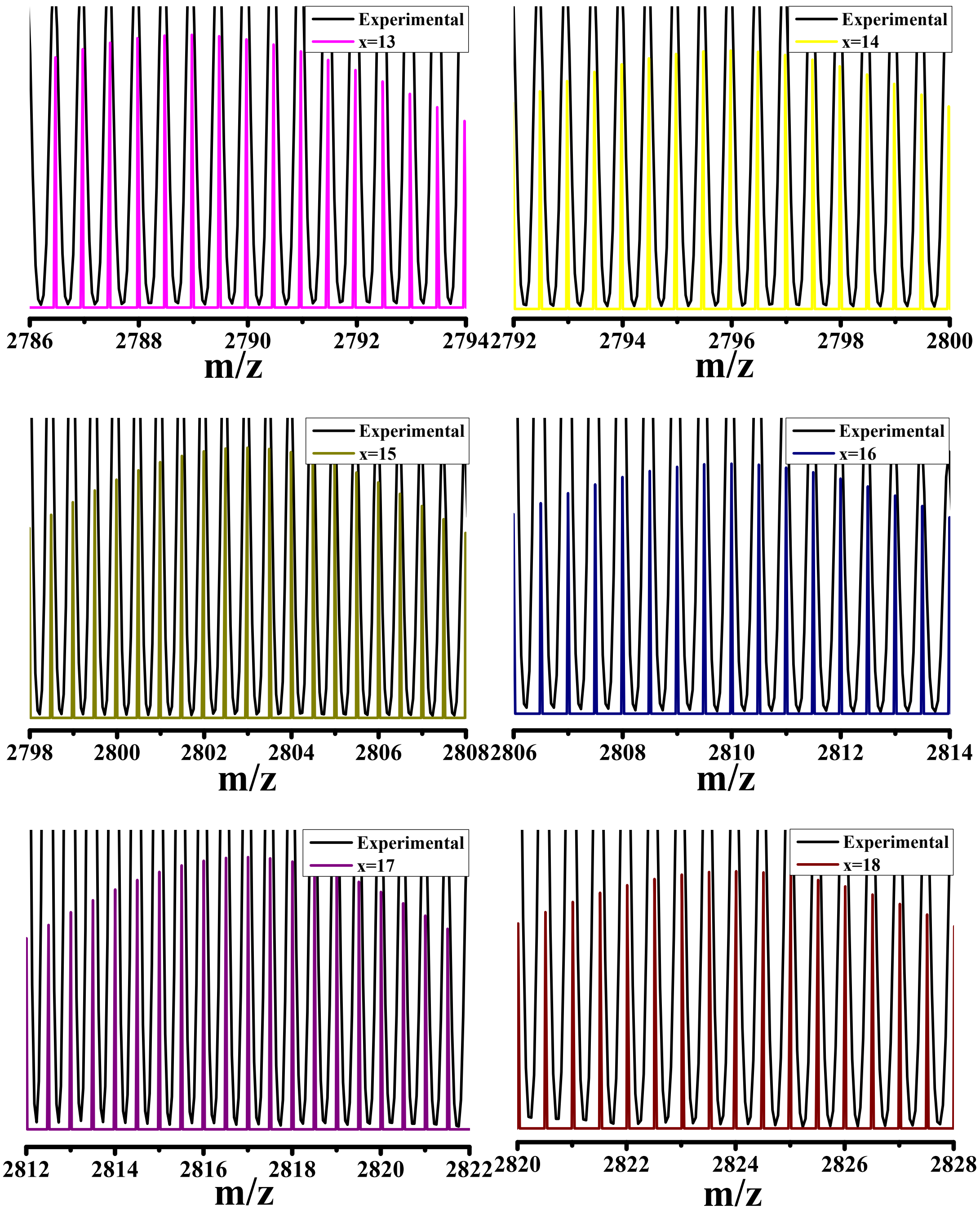

Fig. S10 The partly expanded spectra of of F1 Fragments (coloured: simulated isotope patterns; Black: observed isotope patterns).

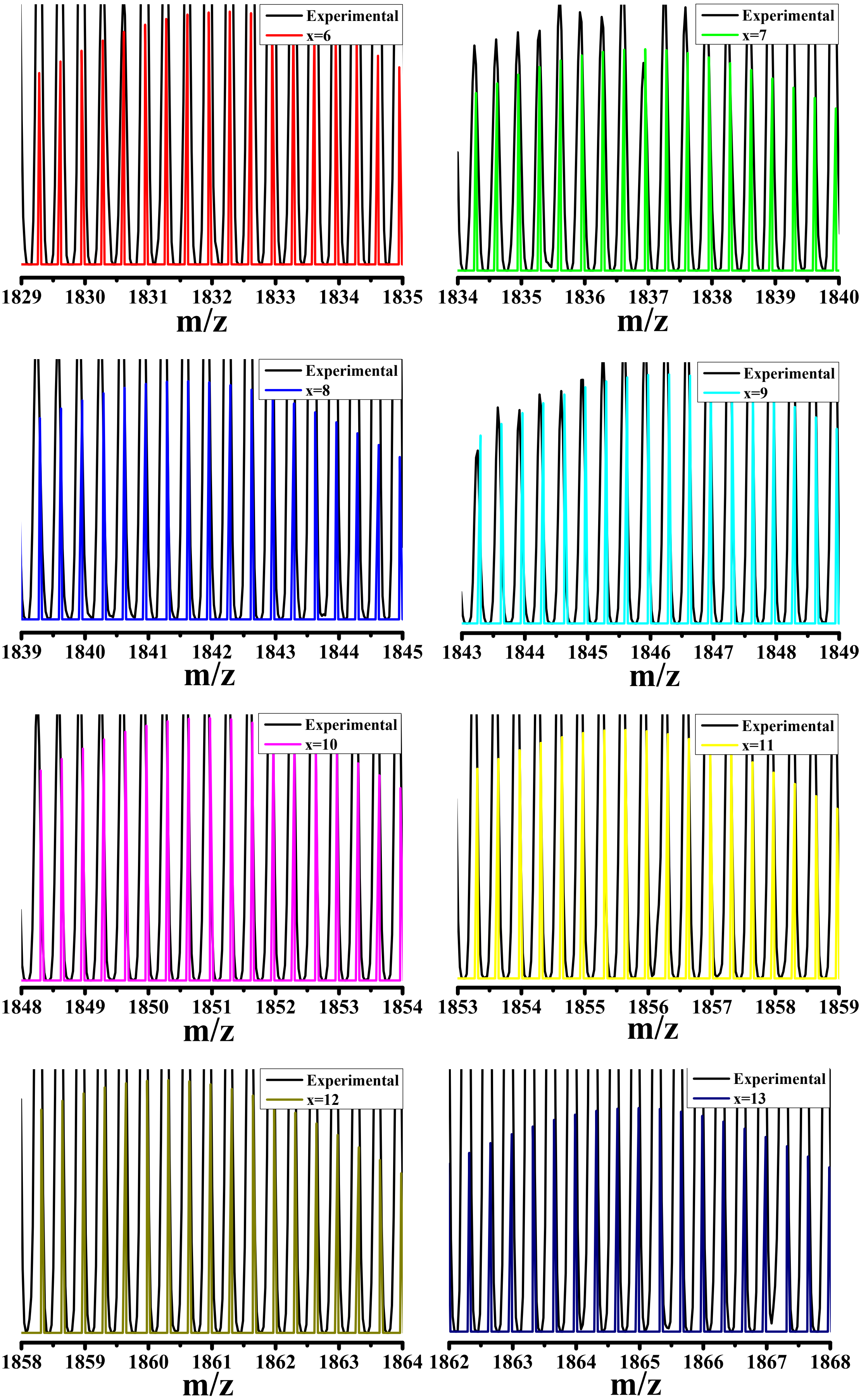
Experimental
x=6
1829 1830 1831 1832 1833 1834 1835
m/z
Experimental
x=7
1834 1835 1836 1837 1838 1839 1840
m/z
Experimental
x=8
1839 1840 1841 1842 1843 1844 1845
m/z
Experimental
x=9
1843 1844 1845 1846 1847 1848 1849
m/z
Experimental
x=10
1848 1849 1850 1851 1852 1853 1854
m/z
Experimental
x=11
1853 1854 1855 1856 1857 1858 1859
m/z
Experimental
x=12
1858 1859 1860 1861 1862 1863 1864
m/z
Experimental
x=13
1862 1863 1864 1865 1866 1867 1868
m/z

Fig. S11 The partly expanded spectra of of F2 Fragments (coloured: simulated isotope patterns; Black: observed isotope patterns).

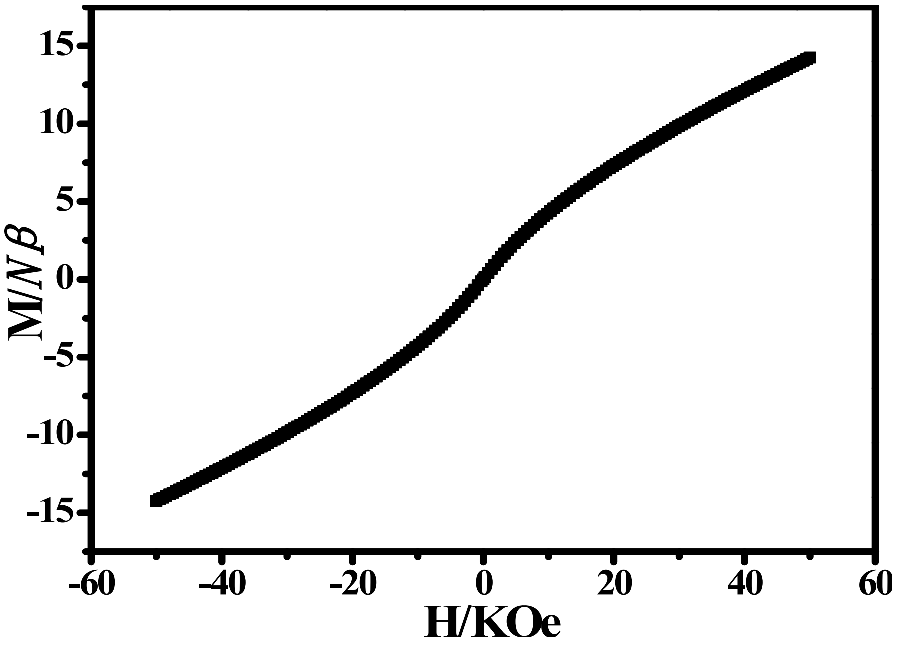

Fig. S12 The M vs H curve of **1** at 2 K.

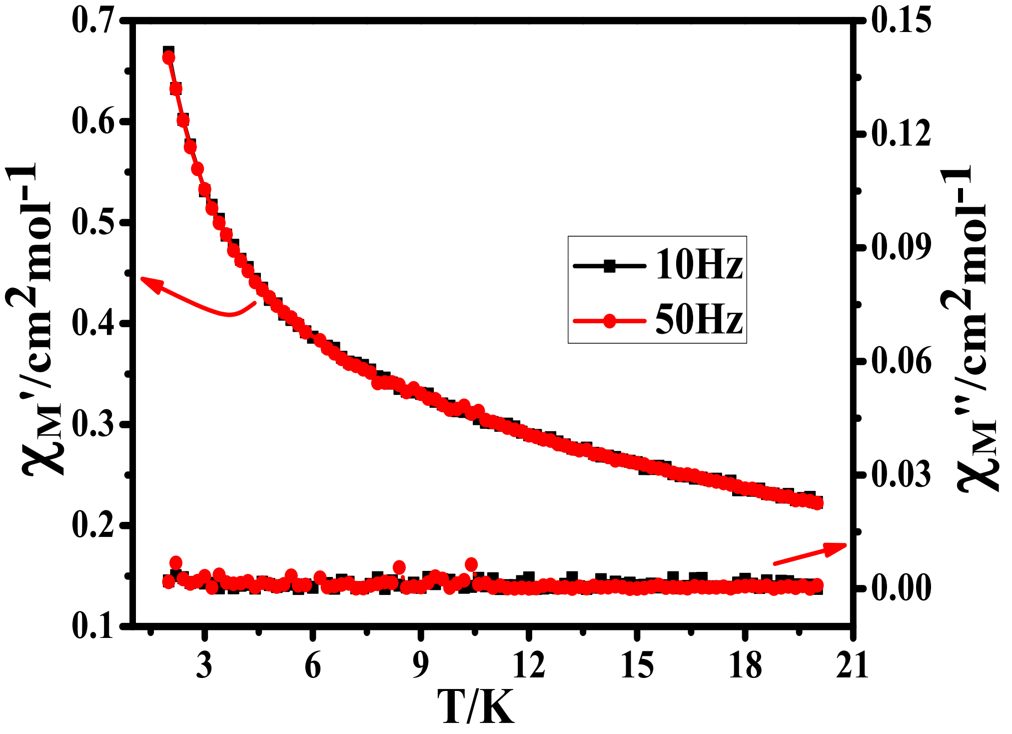

Fig. S13 The temperature dependence of the in-phase (χ_M', up) and the out-of-phase (χ_M'', down) ac magnetic susceptibilities of **1**.